

## Article

## Open Access

# Mineralocorticoid Receptor Pathway Is a Key Mediator of Carfilzomib-induced Nephrotoxicity: Preventive Role of Eplerenone

Panagiotis Efentakis<sup>1</sup>, Sofia Lamprou<sup>1</sup>, Manousos Makridakis<sup>2</sup>, Ioanna Barla<sup>3</sup>, Panagiota-Efstathia Nikolaou<sup>1</sup>, Andriana Christodoulou<sup>1</sup>, Costantinos Dimitriou<sup>2</sup>, Nikolaos Kostomitsopoulos<sup>2</sup>, Ioannis Ntanas-Stathopoulos<sup>4</sup>, Irene Theochari<sup>5</sup>, Maria Gavriatopoulou<sup>4</sup>, Harikleia Gakiopoulou<sup>5</sup>, Androniki Tasouli<sup>6</sup>, Antonia Vlahou<sup>2</sup>, Evangelos Gikas<sup>3</sup>, Nikolaos Thomaidis<sup>3</sup>, Meletios-Athanasios Dimopoulos<sup>4</sup>, Evangelos Terpos<sup>4</sup>, Ioanna Andreadou<sup>1</sup>

**Correspondence:** Ioanna Andreadou (jandread@pharm.uoa.gr).

## ABSTRACT

Carfilzomib is an irreversible proteasome inhibitor indicated for relapsed/refractory multiple myeloma. Carfilzomib toxicity includes renal adverse effects (RAEs) of obscure pathobiology. Therefore, we investigated the mechanisms of nephrotoxicity developed by Carfilzomib. In a first experimental series, we used our previously established *in vivo* mouse models of Carfilzomib cardiotoxicity, that incorporated 2 and 4 doses of Carfilzomib, to identify whether Carfilzomib affects renal pathways. Hematology and biochemical analyses were performed, while kidneys underwent histological and molecular analyses. In a second and third experimental series, the 4 doses protocol was repeated for 24 hours urine collection and proteomic/metabolomic analyses. To test an experimental intervention, primary murine collecting duct tubular epithelial cells were treated with Carfilzomib and/or Eplerenone and Metformin. Finally, Eplerenone was orally co-administered with Carfilzomib daily (165 mg/kg) in the 4 doses protocol. We additionally used material from 7 patients to validate our findings and patients underwent biochemical analysis and assessment of renal mineralocorticoid receptor (MR) axis activation. *In vivo* screening showed that Carfilzomib-induced renal histological deficits and increased serum creatinine, urea, NGAL levels, and proteinuria only in the 4 doses protocol. Carfilzomib decreased diuresis, altered renal metabolism, and activated MR axis. This was consistent with the cytotoxicity found in primary murine collecting duct tubular epithelial cells, whereas Carfilzomib + Eplerenone co-administration abrogated Carfilzomib-related nephrotoxic effects *in vitro* and *in vivo*. Renal SGK-1, a marker of MR activation, increased in patients with Carfilzomib-related RAEs. Conclusively, Carfilzomib-induced renal MR/SGK-1 activation orchestrates RAEs and water retention both *in vivo* and in the clinical setting. MR blockade emerges as a potential therapeutic approach against Carfilzomib-related nephrotoxicity.

## INTRODUCTION

Carfilzomib (Cfz) is an irreversible proteasome inhibitor indicated for relapsed/refractory multiple myeloma (R/R MM). ENDEAVOR study showed that Cfz improves the overall survival of patients with R/R MM compared to the reversible

proteasome inhibitor Bortezomib, whereas it is accounted for higher occurrence of cardiovascular (CVAEs) and renal adverse effects (RAEs).<sup>1</sup> Continuous monitoring of Cfz-treated patients is essential, and clinical management of CVAEs and RAEs is not uniform, because guidelines on preventive measures in patients with Cfz-induced adverse effects are limited.<sup>2</sup>

ENDEAVOR study showed that Cfz-treated patients present grade 1–3 renal complications (acute renal failure, renal failure, renal impairment, acute prerenal failure, anuria, oliguria, and prerenal failure) at higher occurrence (15%–19%) compared to Bortezomib (10%–11%).<sup>1</sup> However, the biology of the observed RAEs is obscure. Cfz-associated renal complications are common, occur acutely and are unpredictable.<sup>3</sup> Cfz-related RAEs involve the manifestation of thrombotic microangiopathy (TMA), albuminuria associated with focal segmental glomerulosclerosis (FSGS) but also histopathological-only findings with no clinical symptoms.<sup>3</sup> Further investigation of Cfz-induced nephrotoxicity is needed to highlight the mechanisms of these complications and discover novel and safe prophylactic therapies.<sup>3</sup>

We have previously established an *in vivo* Cfz-induced cardiotoxicity model that mimics the clinical observations<sup>4</sup> and demonstrated that the observed cardiotoxicity is mediated by a dysregulation of the AMP-activated kinase  $\alpha$

<sup>1</sup>Laboratory of Pharmacology, School of Pharmacy, National and Kapodistrian University of Athens, Greece

<sup>2</sup>Biomedical Research Foundation Academy of Athens, Greece

<sup>3</sup>School of Chemistry, National and Kapodistrian University of Athens, Greece

<sup>4</sup>Department of Clinical Therapeutics, School of Medicine, National and Kapodistrian University of Athens, School of Medicine, Athens, Greece

<sup>5</sup>1st Department of Pathology, School of Medicine, National and Kapodistrian University of Athens, Greece

<sup>6</sup>Onassis Cardiac Surgery Center, Athens, Greece

ET and IA have equally contributed senior authors.

Supplemental digital content is available for this article.

Copyright © 2022 the Author(s). Published by Wolters Kluwer Health, Inc. on behalf of the European Hematology Association. This is an open-access article distributed under the terms of the Creative Commons Attribution-Non Commercial-No Derivatives License 4.0 (CCBY-NC-ND), where it is permissible to download and share the work provided it is properly cited. The work cannot be changed in any way or used commercially without permission from the journal.

HemaSphere (2022) 6:11(e791).

<http://dx.doi.org/10.1097/HS9.0000000000000791>.

Received: July 10, 2022 / Accepted: September 20, 2022

(AMPK $\alpha$ )-autophagy axis in the myocardium.<sup>4</sup> However, in this study, other adverse effects of Cfz were not investigated. Considering that the management of Cfz-induced RAEs remains an unmet clinical need, herein, we sought to investigate the molecular signaling of Cfz-induced nephrotoxicity and to assess possible preventive therapies.

## METHODS

For Complete Materials and Methods please refer to the Suppl. Materials.

### Animals

Eighty-nine male C57Bl/6J (13–14 weeks of age) mice were used in this study. Mice were bred and housed in the Animal Facility of Biomedical Research Foundation Academy of Athens and in accordance with the “Guide for the care and use of Laboratory animals” and experiments were approved by the Ethics Committee (Approval No: 182464;14-05-2019) according to ARRIVE guidelines.<sup>5,6</sup> In the first experimental series, mice were randomized as follows: two-dose protocol: (1) control (NaCl 0.9%), (2) Cfz (8 mg/kg), for 2 consecutive days; four-dose protocol: (1) control (NaCl 0.9%), (2) Cfz (8 mg/kg), for 6 days,<sup>4</sup> (n = 5–6 per group). NaCl and Cfz were injected intraperitoneally daily on the 2-dose protocol and on alternate days in the 4-dose protocol (Figure S1A, B). Cfz regimens were based on our previous study addressing its cardiotoxicity.<sup>4</sup> Briefly, Cfz initial dosing is selected to be 27 or 56 mg/m<sup>2</sup> and can be reduced to 15 mg/m<sup>2</sup> upon manifestation of life-threatening CVAEs, before medication discontinuation. In a translational scope, the dose regimen selected for the 2-dose protocol is equivalent to a human equivalent dose (HED) of 14.85 mg/m<sup>2</sup> which is the lowest dose used in MM patients, whereas the dose regimen selected for the 4-dose protocol is equivalent to a HED of 29.65 mg/m<sup>2</sup>, which is within the range of the initial dose of Cfz. Therefore, the dose regimens used in this study are in line with the dose regimens used in humans. However, metabolism and drug clearance in mice differs in comparison with humans; therefore, more frequent administration of Cfz in the murine model is needed to maintain the same proteasome inhibitory effects with the clinical setting.<sup>7</sup>

At the end of the experiments, animals were anesthetized with ketamine (100 mg/kg) and euthanized by cervical dislocation. Whole blood, plasma, and kidney samples were collected. In a second experimental series, the previous experiments were repeated only for the 4-dose protocol (n = 5–6 per group), and blood, sera, and kidney samples underwent biochemical (serum creatine, urea-bound-nitrogen [BUN], lactate Dehydrogenase [LDH], C-reactive protein [CRP], and full blood count), proteomic and western blot analysis. In a third series of experiments, mice were randomized as in the 4-dose protocol (n = 6 per group) and individually housed in metabolic cages in which they were provided with food and water ad libitum for urine collection. Blood, sera, and urine samples were subjected to metabolomic analysis. Finally, in a fourth experimental series mice were randomized as follows: (1) control (NaCl 0.9%), (2) Cfz (8 mg/kg), (3) Eplerenone (165 mg/kg), and (4) Cfz (8 mg/kg) (4 dose) + Eplerenone (165 mg/kg) administered for 6 days (Figure S1C) (n = 6 per group). Eplerenone dose was calculated based on the interspecies dose conversion formulas which corresponds to a low dose of Eplerenone at a HED of 25 mg and in compliance with the literature.<sup>8</sup> Molecular, renal histology and biochemical analyses were performed, whereas in a fifth experimental series the experiments were repeated for metabolomic analyses (n = 6 per group).

### Patients

Herein, we report data for 7 R/R MM patients who were treated with Cfz-based regimens in the Department of Clinical Therapeutics, Medical School, National and Kapodistrian University of Athens and presented with Cfz-related RAEs.

Patients were closely monitored and evaluated for renal complications and renal biopsies were obtained upon manifestation of nephrotoxicity. RAEs related to myeloma progression were not rated as Cfz-related. RAEs were rated according to National Cancer Institute Common Terminology Criteria for Adverse Events, v4.03. Approval was obtained from the institutional review board/Ethics Committee of the hospital. Patients' clinical characteristics are presented in Table 1 and renal biopsies characteristics are presented in Table S1. Renal biopsies originating from macroscopically healthy parenchyma from 3 patients who underwent nephrectomy due to other reasons unrelated to MM or Cfz treatment were used as Control samples. The estimated glomerular filtration rate (eGFR, mL/min/1.73m<sup>2</sup>) was estimated using the chronic kidney disease epidemiology collaboration formula<sup>9</sup> and biochemical analyses were performed by the Department of Clinical Therapeutics, Medical School, National and Kapodistrian University of Athens using automated analyzers.

### Statistical analysis

Data are presented as means  $\pm$  standard error (mean  $\pm$  SEM). Continuous variables were compared between 2 groups using an unpaired, 2-tailed, Student's T-Test, among >3 groups using one-way analysis of variance, and post hoc comparisons were made using Tukey's test. For clinical data, Mann-Whitney Test was performed, without assumption of normal distribution of the samples with an unpaired 2-tailed T-Test. No assumption of equal variability of differences was performed and data were corrected with Greenhouse-Geisser correction. A *P*-value of <0.05 was considered statistically significant. All statistical analyses and graph preparation were performed using GraphPad Prism 8.5 analysis software (GraphPad Software, Inc., La Jolla, CA). No outliers due to biological diversity were excluded. The absence of outlying values was confirmed by GraphPad Prism analysis software, using ROUT method and *Q* = 1%.

## RESULTS

### Four doses of Cfz increased serum creatinine and BUN and presented early histological signs of nephrotoxicity

We initially applied our previously established translational protocols of Cfz cardiotoxicity<sup>4</sup> and we monitored biomarkers

**Table 1**  
Patient Clinical Characteristics

<b>Biometrical parameters</b>	
Age, years, median (range)	66 (56–67)
Gender, male/female	71.4%/28.6%
Median baseline eGFR (mL/min/1.73 m <sup>2</sup> ) (range)	69.2 (62.5–89.7)
<b>Comorbidities</b>	
Hypertension	57.1%
Diabetes mellitus	28.6%
Peripheral angiopathy	13.3%
Coronary heart disease	13.3%
<b>MM immunoglobulin type</b>	
$\kappa$ LC	71.40%
$\lambda$ LC	28.60%
Non-secretory	0%
Previous HDM/ASCT	42.90%
<b>Carfilzomib dose (mg/m<sup>2</sup>)</b>	
20/27	44%
20/36	13.3%
20/56	42.9%
Carfilzomib-dexamethasone (Kd)	73%
Kd+ Lenalidomide (KRd)	13.3%
Other Cfz combinations	13.3%

Cfz = Carfilzomib; eGFR = estimated glomerular rate; HDM/ASCT = high-dose melphalan therapy with autologous stem cell transplantation; MM = multiple myeloma;  $\kappa$ LC = kappa light chain;  $\lambda$ LC = lambda light chain.

of renal impairment, such as serum creatinine, BUN, and LDH. We observed that 2 doses of Cfz did not inhibit renal proteasome activity and did not lead to a significant increase of serum creatinine or BUN, while significantly increased LDH and circulating neutrophils (Figure S2A–E). No noteworthy histological deficits were reported, while an infiltration of immune cells (ICs) was observed only in the Cfz group (Figure S2F–G). On the contrary, 4 doses of Cfz, led to an increase of serum creatinine and BUN (Fig. 1A, B) and successfully inhibited renal proteasome activity (Fig. 1C) additionally to the inhibition of

proteasome activity in the peripheral blood mononuclear cells (PBMCs), as previously shown at the same dose.<sup>4</sup> This increase in serum creatinine and BUN was accompanied by a significant increase in LDH and circulating total white blood cells (WBCs) and neutrophils (Fig. 1D, E). Four doses of Cfz led to a significant Lcn2 (NGAL) mRNA increase without changes in Kidney injury molecule-1 mRNA expression (Fig. 1F), which are 2 sensitive renal injury markers,<sup>10</sup> and to histological deficits such as glomerular volume increase and juxtaglomerular apparatus hyperplasia (JAH), mild IC infiltration and fibrosis (Fig. 1G–J).

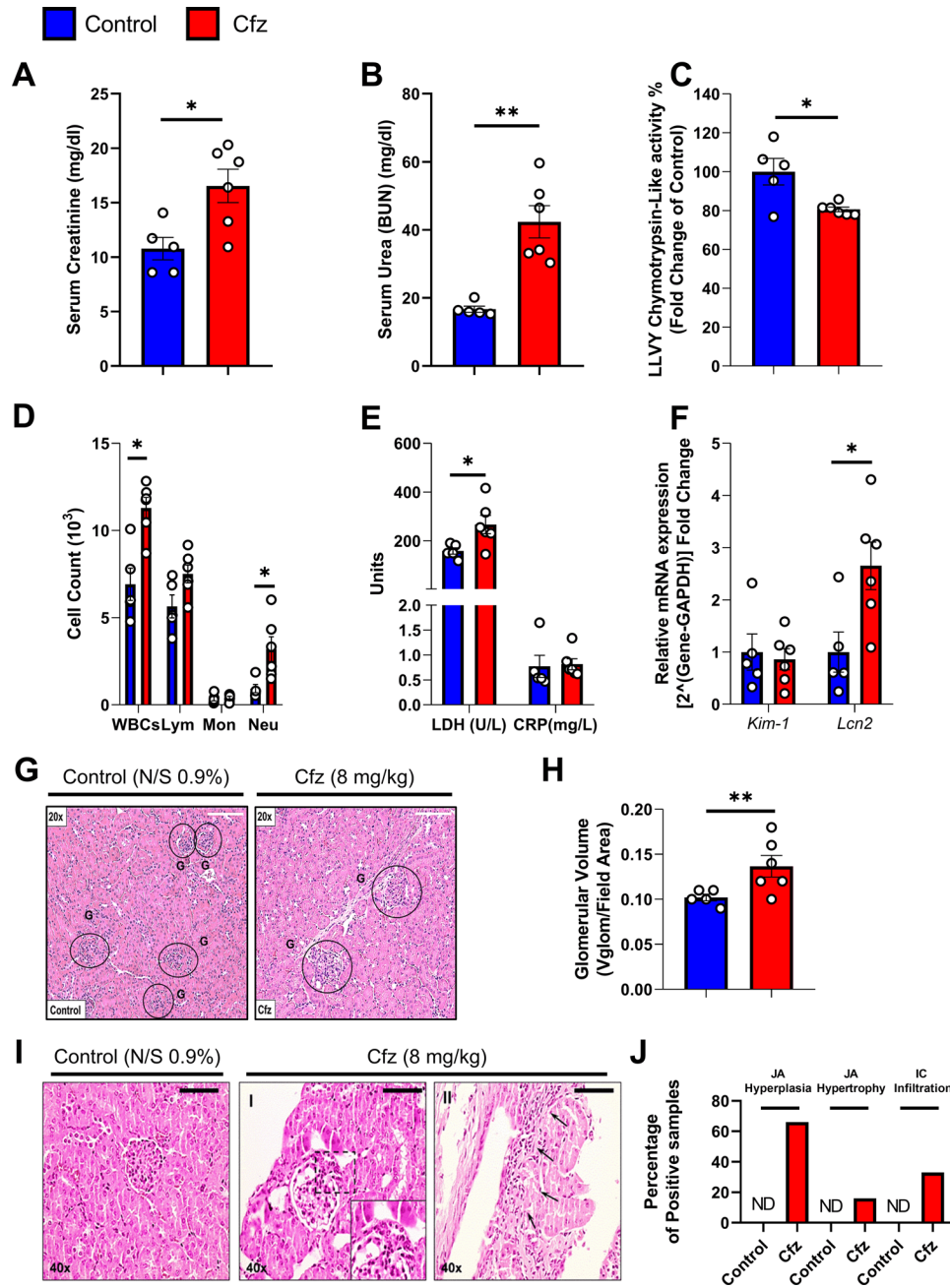


**Figure 1. Four doses of Carfilzomib increased serum creatinine, urea-bound-nitrogen (BUN), LDH, and circulating white blood cells and neutrophils. Early histological signs of nephrotoxicity.** Graphs of (A) serum creatinine (mg/dL), (B) serum BUN (mg/dL) (n = 5–6 per group) and (C) renal % LLVY chymotrypsin-like activity expressed as fold change of control (n = 5–6 per group). (D) Total blood cell count ( $\times 10^3$  cells) (n = 5–6 per group) and (E) graph of lactate dehydrogenase (LDH, U/L) and C-reactive protein (CRP, mg/L) (n = 5–6 per group). (F) Relative mRNA expression of Kim-1 and Lcn2 expressed as fold change of controls (n = 5–6 per group). (G) Representative hematoxylin-eosin histology images of kidney tissue and (H) graphs of glomerular volume (Vglom/field area) (20 $\times$ , bar corresponds to 20  $\mu$ m). (I) Representative hematoxylin-eosin histology images of kidney tissue and (J) graph percentage of positive samples presenting juxtaglomerular apparatus (JA) hyperplasia, hypertrophy, and immune cell (IC) infiltration (n = 5–6 per group; 40 $\times$ , bar corresponds to 15  $\mu$ m). Blue scatter bars refer to the control and red scatter bars refer to Cfz groups. Data are presented as mean  $\pm$  SEM. Student’s T-Test, unpaired, 2-tailed. \* $P < 0.05$ , \*\* $P < 0.01$ .



Since increased serum creatinine, BUN, LDH,<sup>3</sup> NGAL,<sup>10</sup> glomerular volume,<sup>11</sup> and JAH<sup>12</sup> are all implicated with renal injury in clinical settings, we established an initial interconnection of Cfz 4 doses administration and renal dysfunction and subsequently proceeded to the investigation of the molecular mechanism, through unbiased proteomic analysis.

#### Metabolic, protein repair, and molecular transport pathways are differentially regulated by Cfz in the kidneys: emerging role of AMPK $\alpha$

To investigate, in an unsupervised manner, the underlying signaling that is induced by Cfz in the kidneys we performed liquid chromatography-mass spectrometry/mass spectrometry (LC-MS/MS) proteomic analysis. In the multivariate principal component analysis (PCA), Control and Cfz samples were successfully separated in the first component ( $\tau_1$ ; Fig. 2A). Pathway enrichment analysis of the statistically significant or differentially expressed proteins revealed that protein repair, mitochondrial and non-mitochondrial metabolic, and endoplasmic reticulum-stress-related pathways are implicated in Cfz's renal effect. Additionally, vascular endothelial growth factor receptor 2 (VEGFR2) related vascular permeabilization, platelet activation and aggregation, embryonic lethal abnormal visual protein (ELAV)-protein 1 (HuR), and apoptosis execution pathways were also found to be affected (Fig. 2B). We subsequently focused on surrogate markers of the significant proteomic pathways through western blot analysis.

We found that—as far as protein repair and autophagy are concerned—Cfz did not lead to any changes in mammalian target of rapamycin (mTOR) or Regulatory-associated protein of mTOR (Raptor) expression or phosphorylation (Fig. 2C). However, Cfz led to a decreased phosphorylation of AMPK $\alpha$  and an increase in autophagy marker microtubule-associated proteins 1A/1B light chain 3B (LC3B) (Fig. 2C). Regarding apoptosis initiation and execution, we observed that Cfz did not affect anti-apoptotic molecules, namely protein kinase B (Akt) phosphorylation or expression and B-cell lymphoma-extra-large (Bcl-xl), while increased pro-apoptotic Bcl-2-associated X protein (Bax) expression and decreased apoptosis-executive molecule cleaved caspase 1. The latter indicate a possible apoptosis initiation that does not progress into apoptosis execution at the investigated timepoint (Fig. 2D). Taking into account that HuR pathway is implicated with oxidative stress- and inflammatory-dependent progression of kidney diseases,<sup>13</sup> we investigated oxidative stress- and inflammation-related pathways. We found that nuclear factor  $\kappa$  beta (NF- $\kappa$ B) and manganese superoxide dismutase (MnSOD) expression remained unchanged, whereas NF- $\kappa$ B phosphorylation was decreased. However, inducible nitric oxide synthase (iNOS) expression was significantly upregulated by Cfz, which can be related with the mild IC infiltration observed in the kidneys of the Cfz-treated mice (Figs. 1I, J and 2E). In line with increased iNOS expression and IC infiltration, we validated the increased VEGFR2 expression, which is associated with increased vascular permeability.<sup>14</sup> However, endothelial cell homeostasis functional markers such as endothelial nitric oxide synthase (eNOS) expression and phosphorylation and vascular endothelial growth factor A (VEGF-A) expression remained unchanged (Fig. 2F).

Since platelet activation and aggregation, metabolism, and transport of molecules also emerged as significant pathways from proteomics data (Fig. 2B), we subsequently focused our interest on these additional pathways.

#### Cfz did not induce TMA in the in vivo murine model

Since TMA is highly implicated with Cfz's RAEs<sup>3</sup> we investigated platelet homeostasis and von Willebrand factor (vWF)-cleaving protease (ADAM-TS13) activity—a diagnostic marker of TMA<sup>15</sup> and vWF cleavage in the blood. We found that 4 doses of Cfz did not lead to changes in platelet number

but led to decreased platelet distribution width (PDW) (Figure S3A). Decreased PDW is associated with decreased platelet activity and thus decreased thrombogenicity.<sup>16</sup> Moreover, Cfz led to an increased ADAM-TS13 activity and increased cleavage of vWF (Figure S3B-D). Since TMA is associated with decreased ADAM-TS13 activity, which leads to decreased vWF cleavage,<sup>17</sup> it seems that TMA does not contribute to the molecular mechanism of Cfz's nephrotoxicity in mice. Therefore, we subsequently focused on the other identified, differentially regulated pathways, namely metabolism and transport of molecules.

#### Cfz led to water retention and metabolic alterations in the kidneys, plasma, and urine in vivo

To investigate the metabolic profile of the Cfz-treated mice, we accommodated them in metabolic cages for 24 hours, with free access to water and food. We observed that 4 doses of Cfz led to a statistically significant decrease in body weight and in urine volume and an increase in 24 hours protein concentration, indicating the manifestation of proteinuria, which is an additional indicator of Cfz-induced nephrotoxicity.<sup>3</sup> Water, food intake, and feces weight remained unaltered (Fig. 3A-F). Hydrophilic interaction chromatography-MS metabolomic analysis revealed that metabolic profile primarily of the Cfz-treated kidneys, but also urine and plasma were successfully separated in the PCA multivariate analysis (Fig. 3G). Pathway enrichment analysis of the metabolites revealed that taurine/hypotaurine metabolism, bile acid biosynthesis, and amino-acids metabolism are differentially regulated by Cfz in the kidneys, whereas glycerophospholipid metabolism and nicotinate and nicotinamide metabolism were additionally differentially regulated by Cfz in the urine and plasma respectively (Fig. 3H). Changes in taurine/hypotaurine metabolism relate to dysregulation of renal osmolarity,<sup>18,19</sup> pointing towards changes in transport of anion and molecules in the kidneys, in line with the proteomic data. Taking together the decreased diuresis induced by Cfz, and collectively the metabolic and proteomic data, we thereupon investigated the mechanisms of water/salt reabsorption in the kidneys.

#### Cfz increased collecting duct transporter gene expression and activated mineralocorticoid receptor signaling, independently of Renin-Angiotensin-Aldosterone axis

Initially, we focused on the primary axis inducing water reabsorption in the kidneys, the Renin-Angiotensin-Aldosterone System (RAAS). We found that 4 doses of Cfz did not activate RAAS, as shown by the unchanged levels of angiotensin-converting enzyme (ACE) activity and angiotensin II (AngII) levels in the sera. Moreover, aldosterone levels were found to be decreased in the serum and without any significant changes in 24 hours aldosterone excretion as assessed in the urine (Fig. 4A-D). The latter might indicate a negative feedback loop on Aldosterone biosynthesis that was herein not investigated. Taking under consideration that AMPK $\alpha$  plays a key transcriptional role in the kidneys, by regulating numerous transporters' gene expression in the proximal tubules, Henle loop, and collecting duct<sup>20</sup> and since we already found that AMPK $\alpha$  phosphorylation is decreased in the kidneys of the Cfz-treated mice (Fig. 2C), we thereupon investigated the gene expression of AMPK $\alpha$  down-stream targets in the kidneys. We found that gene expression of transporters in the proximal tubules (Na<sup>+</sup>-glucose cotransporter 1; Sglt1 and Sodium/proton exchanger 1; Nhe1) and Henle loop (Na<sup>+</sup>-K<sup>+</sup>-Cl<sup>-</sup> cotransporter 2; Nkcc2) remained unchanged, whereas gene expression of transporters in the collecting duct (epithelial sodium channel beta;  $\beta$ -Enac, urea transporter-1 Uta1) and the ubiquitously expressed Sodium-Potassium ATPase (Na<sup>+</sup>-K<sup>+</sup>-ATPase) were significantly increased in the Cfz group (Fig. 4E). Since collecting duct epithelium and especially  $\beta$ -ENaC are key mediators of Na<sup>+</sup> reabsorption,<sup>21</sup> while Na<sup>+</sup> reabsorption and Na<sup>+</sup> gradient are involved with



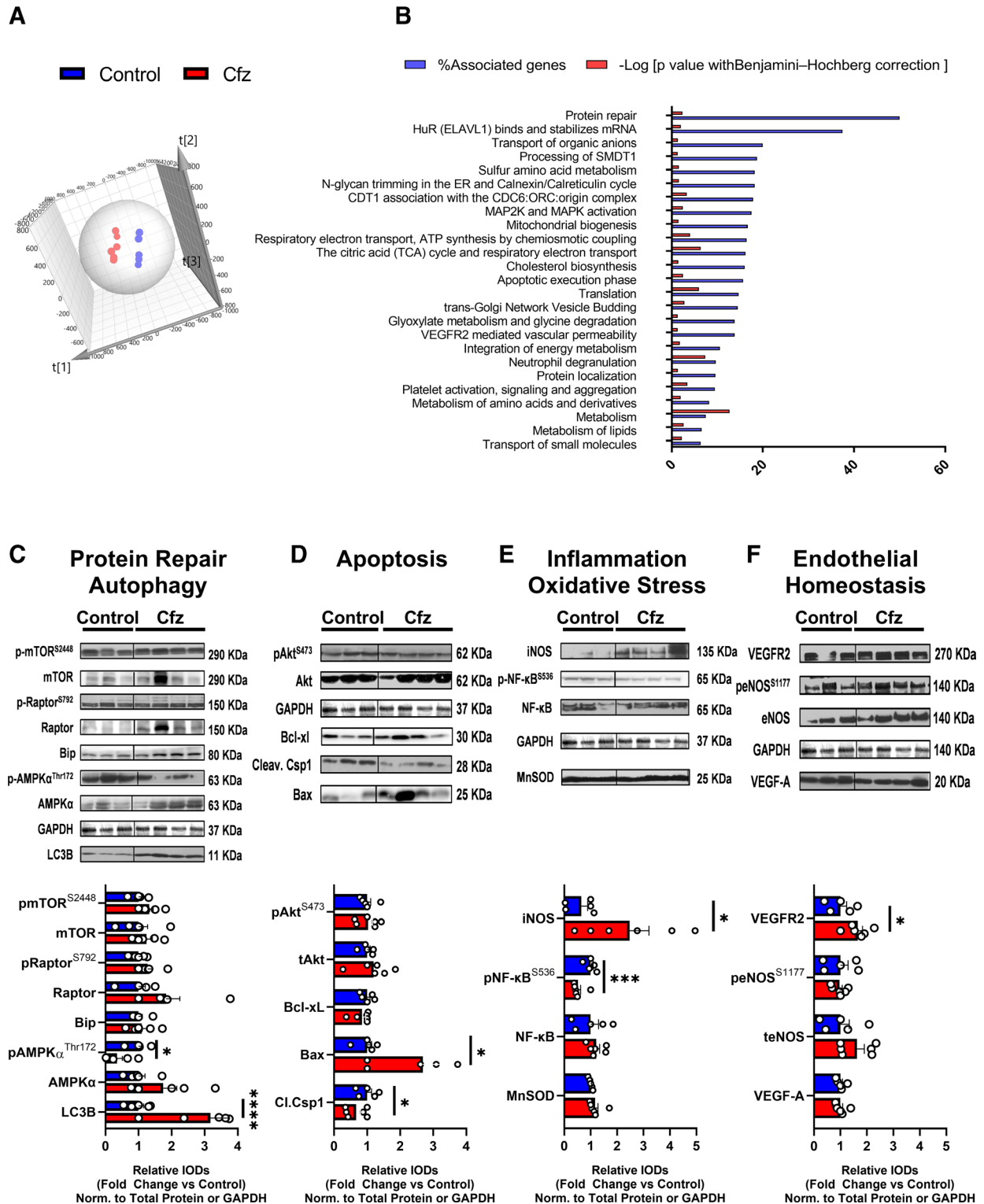


**Figure 2. Metabolic, protein repair, and molecular transport pathways are differentially regulated by Carfilzomib in the kidneys. Emerging role of AMPK $\alpha$ .** (A) Three-dimensional representation of principal components analysis (PCA) of the proteomic analysis ( $R^2 = 0.989$ ;  $F^2 \times \alpha_1 = 0.070$ ). (B) Grouped graph of % associated genes (blue bar) and  $-\log P$  value corrected with Benjamini–Hochberg test (red bar) regarding the significantly or/and differentially regulated proteins in the kidneys ( $n = 5-6$  per group). (C–F) Representative Western blot images and relative densitometry analysis of protein repair-autophagy, apoptosis, inflammation-oxidative stress, and endothelial homeostasis-related pathways. Blue scatter bars refer to the control and red scatter bars refer to Czf groups ( $n = 5-6$  per group). Lines on the representative Western blot images facilitate the separation of groups/samples which were assessed on the same SDS-PAGE gel. All phosphorylated proteins are normalized to their respective total proteins and total proteins are normalized to GAPDH (loading control). Data are presented as mean  $\pm$  SEM. Student's T-Test, unpaired, 2-tailed. \* $P < 0.05$ , \*\*\* $P < 0.005$ . Akt = protein kinase B; AMPK $\alpha$  = AMP-activated kinase  $\alpha$  subunit; Bax = Bcl-2-associated X protein; Bcl-xL = B-cell lymphoma-extra-large; Cl.Casp1 = cleaved caspase 1; eNOS = endothelial nitric oxide synthase; iNOS = inducible nitric oxide synthase; LC3B = microtubule-associated protein 1A/1B light chain 3B; MnSOD = manganese superoxide dismutase; mTOR = mammalian target of rapamycin; NF- $\kappa$ B = nuclear factor kappa-light-chain-enhancer of activated B cells; Raptor = regulatory-associated protein of mTOR; VEGF-A = vascular endothelial growth factor A; VEGFR2 = vascular endothelial growth factor receptor 2.

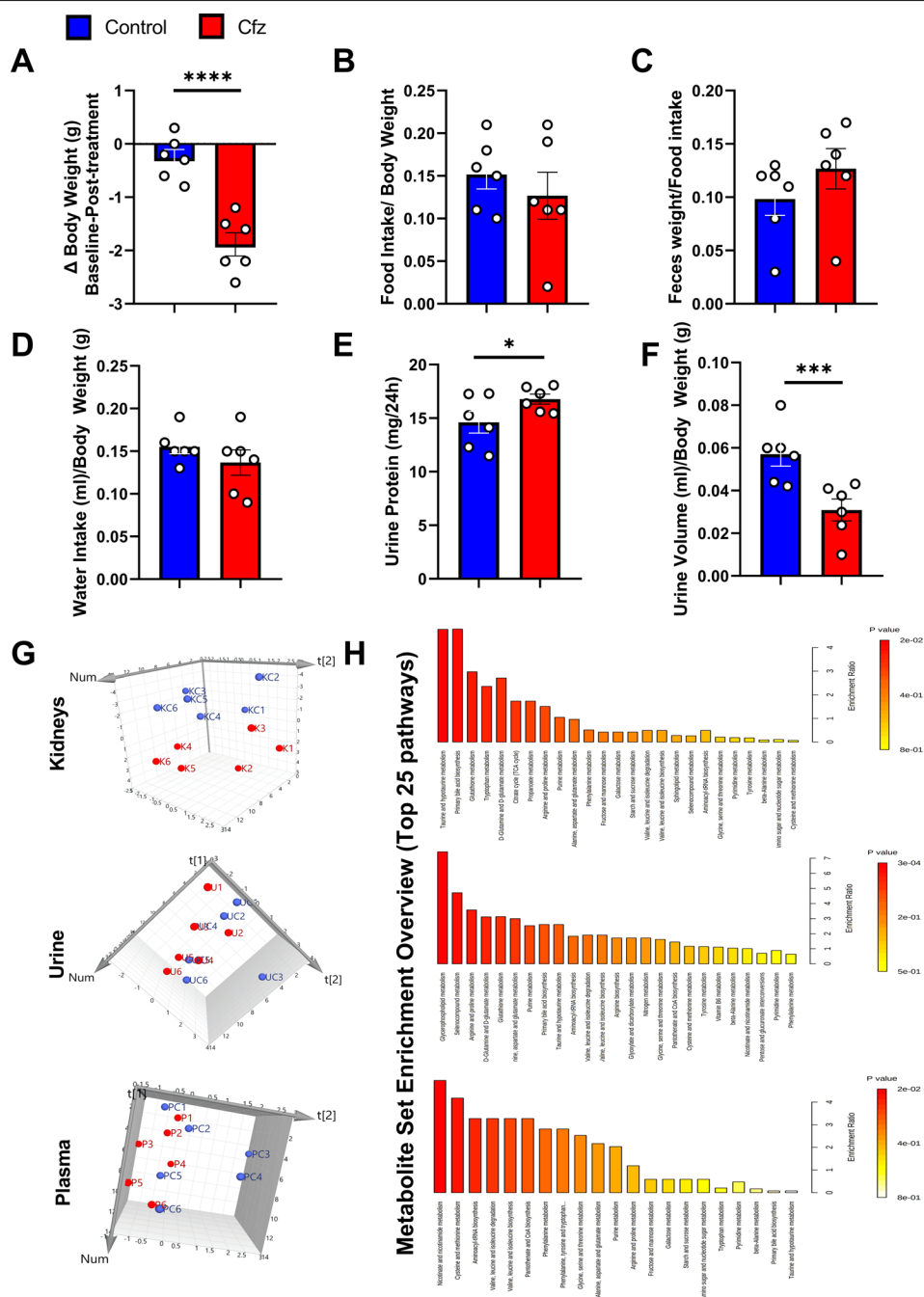


**Figure 3. Four doses of Carfilzomib led to decreased diuresis and to metabolic alterations in the kidneys, plasma, and urine in vivo.** Graphs of metabolic parameters assessed in the metabolic cages after 24 h: (A) body weight (g) change ( $\Delta$  body weight), (B) food intake/body weight, (C) feces weight/body weight, (D) water intake (ml)/body weight(g), (E) urine protein excretion (g/24h) and (F) urine volume (mL)/body weight(g) ( $n = 6$  per group). (G) Three-dimensional representation of principal components analysis (PCA) of the proteomic analysis of the kidney's urine and plasma ( $n = 6$  per group) and (H) metabolite enrichment overview of the top 25 metabolic pathways as emerged from the metabolomic analysis and MetaboAnalyst 5.0 software with enrichment and  $P$  value ascension. Blue scatter bars refer to the Control and red scatter bars refer to Cfz groups. Data are presented as mean  $\pm$  SEM. Student's T-Test, unpaired, 2-tailed. \*\*\* $P < 0.005$ , \*\*\*\* $P < 0.001$ .

mineralocorticoid receptor (MR) activation, we focused our interest on the MR signaling. We found an upregulation of  $\beta$ -ENaC expression in whole kidney lysates (Fig. 4F, G), while in the subcellular fractionation experiments, we found an upregulation of MR in the nucleus, an upregulation of neural precursor cell expressed developmentally down-regulated protein 4 (NEDD-4) and an increased phosphorylation and expression of Serum/Gluocorticoid-Regulated Kinase 1 (SGK-1) in the cytosol (Fig. 4F, H, J). Moreover, the MR cytosolic/nuclear

expression ratio was found to be decreased in the Cfz group, indicating a translocation of the receptor to the nucleus and thus increased MR activity (Fig. 4F, I).<sup>22</sup> Collectively our data suggest that Cfz increased collecting duct transporters mRNA expression and activated MR/SGK-1 signaling in the kidneys, independently of RAAS activation. Since MR activation is implicated with  $\text{Na}^+$  reabsorption and  $\text{K}^+$  sparing from the urine,<sup>23</sup> we further confirmed our finding by measuring plasma and urine electrolytes, collected from the metabolic cages. We

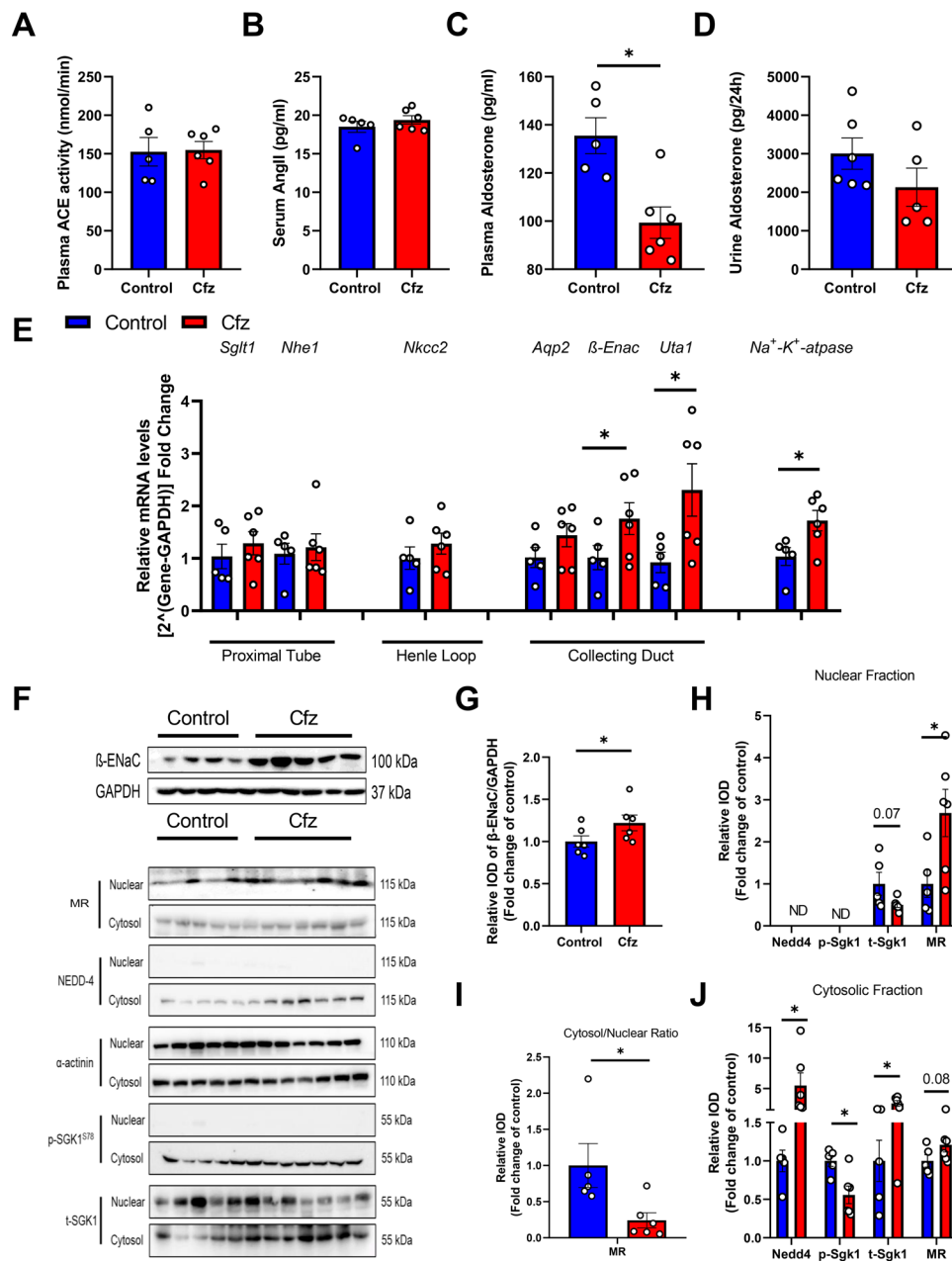


**Figure 4. Carfilzomib increased collecting duct transporters gene expression and activated mineralocorticoid receptor signaling, independently of renin-angiotensin-aldosterone axis.** Graphs of (A) plasma angiotensin-converting enzyme (ACE) activity (nmol/min, n = 10 per group), (B) serum angiotensin II (AngII, n = 5 per group), (C) Plasma aldosterone (pg/mL, n = 5–6 per group) and (D) urine aldosterone excretion (pg/24h, n = 5–6 per group). (E) Graph of relative mRNA levels expressed as fold change of controls of Sglt1, Nhe1, Nkcc2, Aqp2, β-Enac, Uta1, Na-K-atpase in the kidneys (n = 5–6 per group). (F) Representative Western blot images and (G–J) relative densitometry analysis of mineralocorticoid receptor (MR)-SGK-1 related proteins in the cytosolic and nuclear fractions of the kidneys (n = 5–6 per group). Data are presented as mean ± SEM. All phosphorylated proteins are normalized to their respective total proteins and total proteins are normalized to GAPDH or α-actinin (loading controls) Student’s T-Test, unpaired, 2-tailed. \*P < 0.05. Aqp2 = aquaporin 2; β-ENaC = epithelial sodium channel ENaC beta subunit; MR = mineralocorticoid receptor; NEDD4 = neural precursor cell expressed developmentally down-regulated protein 4; Nhe1 = sodium-hydrogen antiporter 1; Nkcc2 = Na-K-Cl cotransporter; Sglt1 = sodium-glucose cotransporter 1; SGK-1 = serum and glucocorticoid-regulated kinase 1; Uta1 = urea transporter A1.

found that 4 doses of Cfz did not lead to any electrolyte imbalance in the plasma, whereas it induced a significant decrease in Na<sup>+</sup> content—indicating water/salt retention—and Na<sup>+</sup>:K<sup>+</sup> ratio in the urine with a parallel increase in urinal K<sup>+</sup> content. The latter confirms our mechanistic hypothesis for MR/SGK-1 activation by Cfz (Table S2). All the above pathways are implicated with water/salt retention, increase of pre-load and arterial blood pressure, adverse phenomena commonly observed in the Cfz-treated patients.<sup>1,24</sup> To investigate the effect of MR/SGK-1 activation on blood pressure in vivo, we assessed systolic blood pressure (SBP) and heart rate (HR) in

the 2- and 4-dose protocols. We found that SBP was increased only in the 4-dose protocol, in which renal MR/SGK-1 axis is shown to be activated in line with the presence of nephrotoxicity, whereas SBP remained unchanged in the 2-dose protocol (Figure S4A-D). Thus, the increased blood pressure in the 4-dose protocol complements our findings on MR/SGK-1 derived phenotype in vivo. Subsequently, we focused on discovering a potent prophylactic therapy, based on our molecular mechanism findings. Therefore, we performed preliminary experiments on primary murine collecting duct tubular epithelial cells (PrCDTECs).



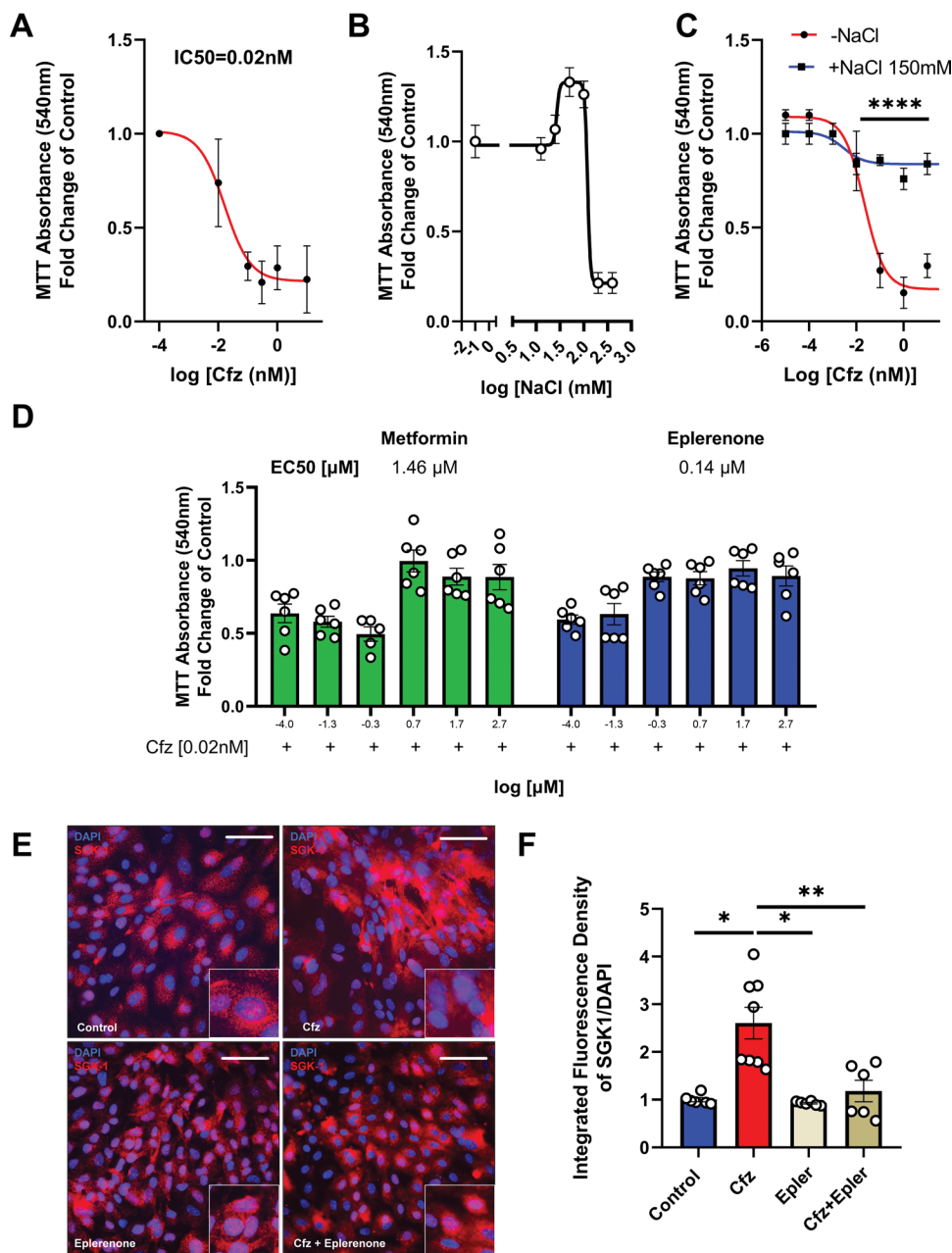


**Figure 5. Eplerenone preponderantly inhibited Carfilzomib-induced cytotoxicity in primary murine collecting duct tubular epithelial cells (PrCDTECs) compared to Metformin and normalized SGK-1 expression.** Graphs of MMT viability assay and IC<sub>50</sub> calculations of PrCDTECs treated with (A) Carfilzomib (IC<sub>50</sub> = 0.02 nM), (B) sodium chloride (NaCl) and (C) Carfilzomib in presence or absence of NaCl (150 mM) and (D) Carfilzomib (0.02 nM) and Metformin or Eplerenone (n = 6 per group). (E–F) Representative immunofluorescence images of PrCDTECs stained with anti-SGK-1 antibody (red) and DAPI (blue) and integrated fluorescence density of SGK-1/DAPI (n = 6–8 per group; 60×, bar corresponds to 20 μm). Data are presented as mean ± SEM. One-way ANOVA, Tukey's post hoc test. \*P < 0.05, \*\*P < 0.01.

#### Eplerenone preponderantly inhibited Cfz-induced cytotoxicity on PrCDTECs compared to Metformin and normalized SGK-1 expression

Initially, we identified the IC<sub>50</sub> of Cfz in PrCDTECs, by performing the cellular viability assay, MTT (Fig. 5A). To investigate whether Na<sup>+</sup> is important in Cfz cytotoxicity, we initially investigated the effect of NaCl on PrCDTECs in a range of 12.5–200 mM. We observed that NaCl induces a hormetic effect on PrCDTECs as at low doses it induces PrCDTECs proliferation, whereas at higher doses it induces cytotoxicity, an effect which is in line with the literature (Fig. 5B).<sup>25</sup>

Subsequently we co-incubated the cells with Cfz and NaCl at its IC<sub>50</sub> concentration of 150 mM. We observed that NaCl prevented Cfz-induced cytotoxicity (Fig. 5C). Taking into consideration that Na<sup>+</sup> is an endogenous inhibitor of ENaC,<sup>26</sup> the latter reinforces the hypothesis that Cfz-induced cytotoxicity is MR/SGK-1/ENaC dependent. Thereafter, we identified (1) the significance of MR activation and Na<sup>+</sup> regulation in Cfz-induced nephrotoxicity and (2) the significant decrease in AMPKα phosphorylation, we sought to identify which of the 2 mechanisms is preponderant in managing Cfz renal effects in vitro. Therefore, we treated the cells with Eplerenone, a

clinically relevant MR blocker and Metformin, a clinically used AMPK $\alpha$  activator, at a concentration range of 0.5–500  $\mu$ M.<sup>7,27</sup> We observed that Eplerenone inhibited Czf's cytotoxicity (Half maximal effective concentration; EC<sub>50</sub> = 0.14  $\mu$ M) which was 10-times more effective than Metformin's prophylactic potential (EC<sub>50</sub> = 1.46  $\mu$ M) (Fig. 5D). Eplerenone, at the same dose, inhibited SGK-1 upregulation, which was increased by Czf in line with our previous *in vivo* results (Fig. 5E–F). Therefore, we established that Eplerenone can act as a potential prophylactic therapy against Czf-induced cytotoxicity *in vitro*, which we sought to confirm *in vivo*.

Eplerenone co-administration with Czf prevented the increase in BUN and in Lcn2, urine retention, and histological deficits *in vivo*

Co-administration of Eplerenone and Czf at clinically translational doses, partially prevented the Czf-induced increase in creatinine and abrogated the Czf-induced increase in BUN (Fig. 6A, B), without interfering with Czf's inhibitory effect in proteasome activity neither in the kidneys nor in the PBMCs (Fig. 6C). Concerning the metabolic parameters, Eplerenone maintained diuresis in the co-administration group at the levels of Control (Fig. 6D), glomerular volume (Fig. 6E, G) and abrogated the Czf-induced increase in kidney injury marker Lcn2

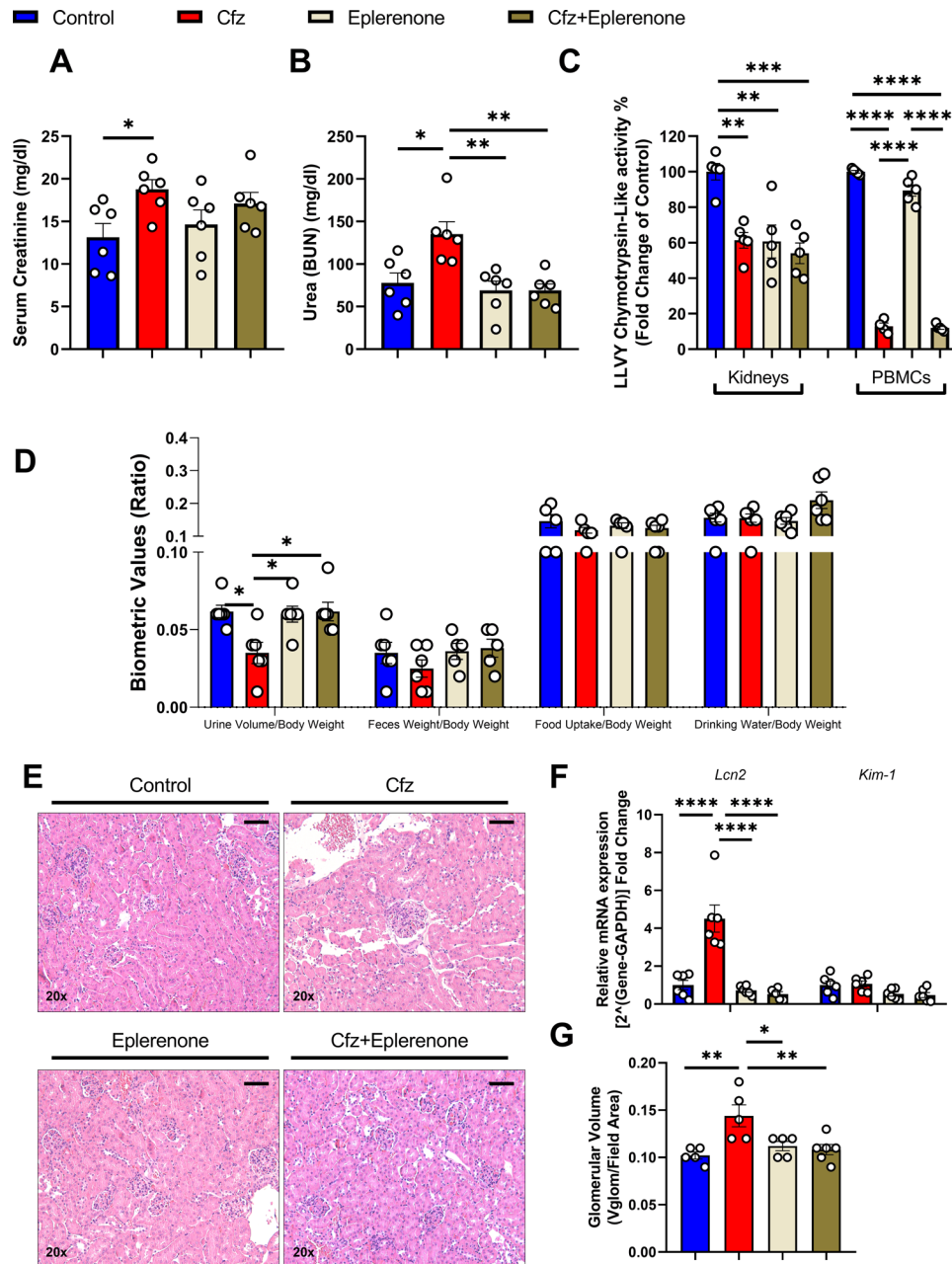


**Figure 6. Eplerenone co-administration with Carfilzomib prevented increase in blood pressure and Lcn2, urine retention, and histological deficits *in vivo*.** Graphs of (A) serum creatinine (mg/dL) and (B) serum urea-bound-nitrogen (BUN) (mg/dL) ( $n = 6$  per group) and (C) % LLVY chymotrypsin-like activity expressed as Fold change of control in the kidneys and peripheral blood mononuclear cells (PBMCs,  $n = 6$  per group). (D) Graphs of metabolic parameters assessed in the metabolic cages after 24 h namely urine volume (mL)/body weight(g), feces weight/body weight, food uptake/body weight and water intake (mL)/body weight(g) ( $n = 6$  per group). (E) Representative hematoxylin-eosin histology images of kidney tissue and (F) relative mRNA expression of Lcn2 and Kim-1 expressed as fold change of controls ( $n = 6$  per group). (G) Graph of glomerular volume (Vglom/field area) (20 $\times$ , bar corresponds to 20  $\mu$ m) ( $n = 5$  per group). One-way ANOVA, Tukey's post hoc test. \* $P < 0.05$ , \*\* $P < 0.01$ .





Analysis (PLS-DA) multivariate analysis in the first principle (t1), while Control, Eplerenone, and Cfz+Eplerenone groups cluster together presenting a similar metabolic profile (Fig. 7C). Pathway enrichment analysis revealed that the same metabolic pathways that discriminated Cfz and Control groups as previously shown (Fig. 3H), discriminated Cfz and Cfz + Eplerenone groups in all analyzed samples, with primary bile acid biosynthesis and taurine/hypotaurine metabolism in the kidneys, glycerophospholipid metabolism in the urine and nicotinate/nicotinamide metabolism in the plasma being the top pathways separating the Cfz and Cfz + Eplerenone groups (Fig. 7D).

MR/SGK-1 axis is upregulated in renal biopsies of patients with Cfz-related RAEs independently of serum creatinine and proteinuria

To solidify our finding in the clinical setting, we recruited 7 RR M/M patients who presented with Cfz-related nephrotoxicity. Two out of 7 (28.6%) patients were classified as IgG<sub>lambda</sub> whereas 5 out of 7 (71.4%) as IgG<sub>kappa</sub> immunoglobulin Myeloma subtype. Their mean age was 66 years of age, while the median time since diagnosis was 6.8 years (Table 1, Table S1). FSGS was found in 44.2% of the glomeruli, compared to the age-corrected physiological range of 18-25%. Fibrosis was found to have affected an average of 24% in the renal cortexes of the patients, whereas 28.6% (2/7 patients) presented TMA in their kidney

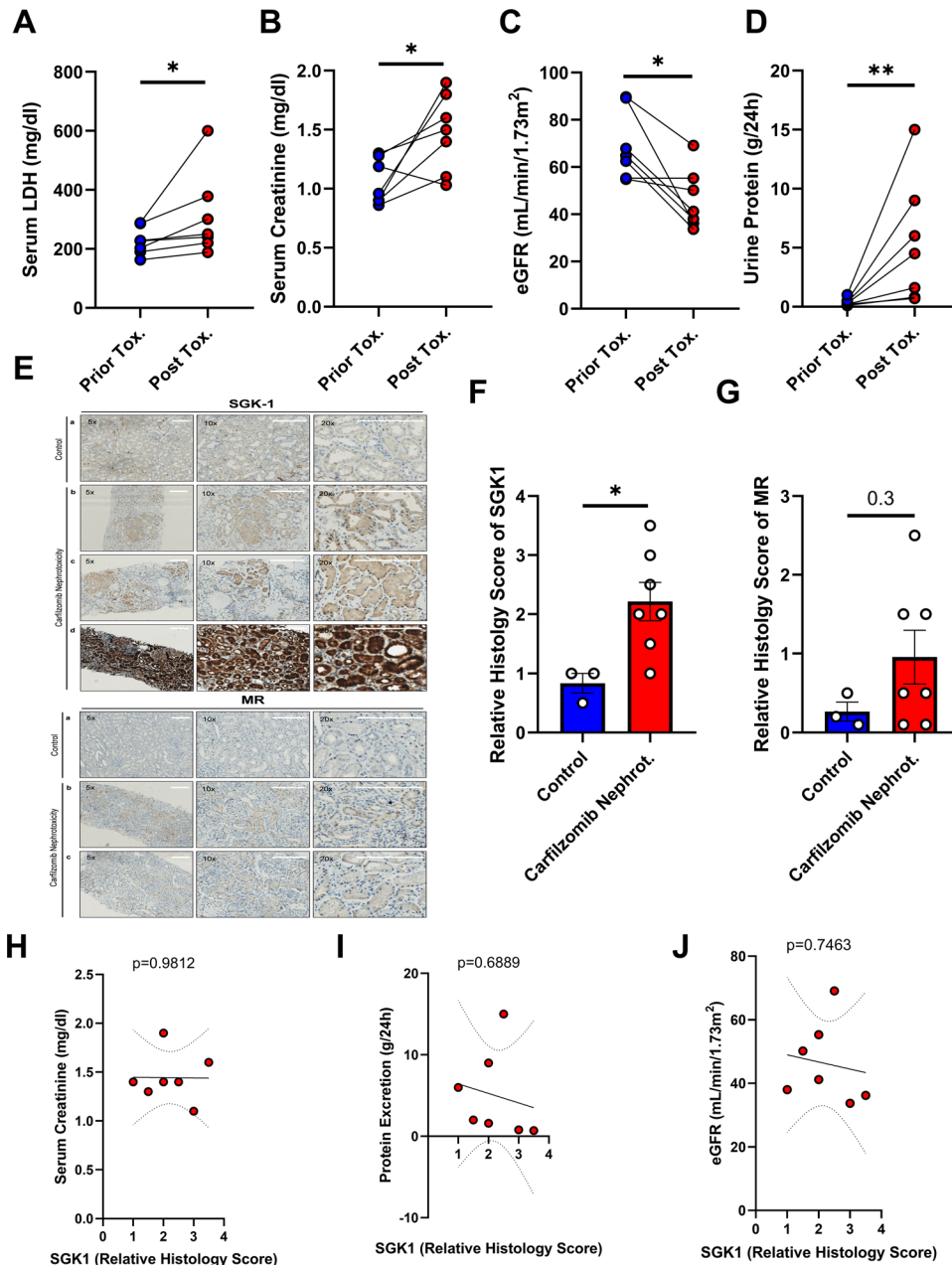


**Figure 8. Carfilzomib nephrotoxicity is presented with increased serum creatinine, LDH concentrations, and proteinuria. SGK-1 is upregulated in renal biopsies of patients with Carfilzomib-related nephrotoxicity.** Graphs of serum (A) serum LDH (mg/mL), (B) creatinine (mg/mL) and (C) estimated glomerular filtration rate (eGFR, mL/min/1.73m<sup>2</sup>) using the chronic kidney disease epidemiology collaboration (CKD-EPI) formula and (D) urine protein (g/24h) prior (baseline, start of therapy) and post-Carfilzomib-induced nephrotoxicity (at the timepoint of clinical presentation of nephrotoxicity) (n = 7 per group). (E) Representative immunohistological stainings of SGK-1 (upper panel) and MR (lower panel) in (a) control renal biopsies and (b–d) Renal biopsies from patients with Carfilzomib-induced nephrotoxicity [(b) low histology score (>1); (c) medium histology score (>2); (d) high histology score (>3); 5x, 10x, and 20x, scale bar represents 200 μm]. (F and G) Graphs of Relative Histology score of SGK-1 and MR expression in the control and Carfilzomib nephrotoxicity renal biopsies (n = 3 and n = 7, respectively). (H–J) Correlation graphs of SGK-1 expression and serum creatine, urine protein, and eGFR, respectively. Mann-Whitney test, paired and unpaired, 2-tailed T-Test, \*P < 0.05, \*\*P < 0.01.

biopsies. Light chain deposition disease was observed in 14.3% (1/7 patients) at the time of the diagnosis of Cfz-related nephrotoxicity (Table S1). Serum LDH, creatinine and Urine protein, and eGFR were found to be increased in the aforementioned patients after manifestation of Cfz-related nephrotoxicity (post-toxicity) compared to their baseline values (prior-toxicity) (Fig. 8A–D). Immunohistological staining of the biopsies revealed that SGK-1 was significantly upregulated in patients with Cfz-related nephrotoxicity, compared to Controls, whereas MR expression was found to be increased by a trend ( $P = 0.3$ ) in the same patients (Fig. 8E–G), in compliance with our *in vivo* data. To identify whether SGK-1 expression was correlated with post-toxicity, we made additional correlation analyses for serum creatinine concentrations, urine protein, and eGFR. We found that SGK-1 was not significantly correlated with any of the 3 parameters (Fig. 8H–J), a fact implying that renal SGK-1 expression can be a novel serum creatinine- and urine protein-independent marker of Cfz-induced nephrotoxicity, which should be validated in a larger cohort of patients.

## DISCUSSION

Cfz is an established therapy against R/R MM; however, Cfz-related CVAEs and RAEs may lead to treatment discontinuation. To date, there are neither prospective studies nor expert consensus on the prevention, monitoring, and treatment of RAEs in myeloma patients treated with Cfz.<sup>28</sup> Cfz-related cardiorenal phenomena seem to be associated with electrolyte imbalance and fluid retention as fluid administration mitigates the cardiovascular and renal complications of the drug.<sup>29,30</sup> However, the effect of Cfz on kidneys and the elucidation of the molecular mechanism of Cfz-induced nephrotoxicity have not been investigated yet.

Herein, for the first time, we have deciphered Cfz's renal effects and we suggest that Cfz-induced activation of MR signaling is implicated with water-salt reabsorption, and urine electrolyte imbalance leading to renal impairment. Cfz-induced renal injury was further supported by the dysregulation of bile acid homeostasis,<sup>31</sup> glycerophospholipid metabolism,<sup>32</sup> and amino-acid metabolism,<sup>33</sup> which are closely related to impaired kidney function and kidney disease. Moreover, we have proven that Cfz-related activation of MR is mediated through increased accumulation of MR and MR-related proteins in the kidneys, leading to the activation of the cascade. Taking into consideration that MR, SGK-1, and  $\beta$ -ENaC proteins physiologically undergo proteasome degradation, administration of the irreversible proteasome inhibitor Cfz possibly leads to decreased degradation of the MR-axis proteins and to a sustained MR-axis activity.<sup>34–37</sup>

Moreover, in the present study we thoroughly investigated pathobiology mechanisms implicated in Cfz's nephrotoxic phenomena, including renal oxidative stress, apoptosis, and incidence of microvascular thrombotic phenomena, such as TMA.<sup>3,38</sup> Regarding apoptosis, we found that Cfz did not resolve in apoptosis execution as it was confirmed by the lack of histological findings of apoptosis in the kidneys. A previous study has shown that Cfz at a dose of 4 mg/kg, twice weekly for 3 weeks increased caspase-3 activity—a marker of apoptosis—in rats.<sup>38</sup> However, the different dose regimen and *in vivo* model can justify the discrepancy in our findings. Noteworthy, in the clinical setting, no signs of histological signs of apoptosis are observed in patients with Cfz-induced nephrotoxicity and nephrotoxic phenomena are usually transient and resolve upon discontinuation of the drug.<sup>39–42</sup> Maladaptive MR signaling and MR sustained activation are already known to induce pathological consequences like extracellular matrix remodeling, apoptosis, or inflammation in the kidneys.<sup>43</sup> Possibly, sustained and maladaptive MR activation by Cfz could later on lead to apoptosis execution in our *in vivo* model.

FSGS is commonly observed in Cfz-treated patients,<sup>3</sup> which is an aftereffect of glomerular hyperplasia and hypertrophy.<sup>44</sup> In our *in vivo* model 4 doses of Cfz-induced glomerular hyperplasia/hypertrophy, a fact that increases the translational value of our findings. Moreover, in the aforementioned rat model of Cfz-induced nephrotoxicity, Cfz-induced renal oxidative stress and increased WBCs number in the circulation.<sup>38</sup> The latter is in agreement with our findings, as we showed that Cfz increased iNOS expression, led to an increase of circulating WBCs and induced renal IC infiltration. However, the renal IC infiltration was also observed in our 2 days protocol, in which no signs of nephrotoxicity were observed. Therefore, despite the fact that oxidative stress is a key pathway in kidney injury and it is also recognized that reactive oxygen species can activate MR signaling,<sup>45,46</sup> we considered it as a secondary mechanism in the Cfz-induced nephrotoxic phenomena.

Concerning TMA, it seems that this mechanism does not contribute to the molecular mechanism of Cfz's nephrotoxicity in mice. The latter comes in agreement with our molecular signaling analysis. TMA is already known to be mediated by increased NF- $\kappa$ B and VEGF activation and expression.<sup>47</sup> On the contrary, in our protocol were found decreased NF- $\kappa$ B phosphorylation and unchanged VEGF expression (Fig. 2E, F), which are contradictory to the pathomechanisms of TMA. Therefore, we subsequently focused on the other identified, differentially regulated pathways, namely metabolism and transport of molecules.

A previous electrophysiology study presented that treatment of renal epithelial cells with proteasome inhibitors, bortezomib, and MG132, led to  $\beta$ -ENaC stimulation, resulting in increased ENaC expression at the cell surface. Proteasome inhibition mimicked SGK-1-dependent stimulation of ENaC by aldosterone. However, the effects of Cfz were not investigated and the observed phenotype was not associated with the drug-related RAEs.<sup>48</sup> The latter study is in complete agreement with our *in vivo* findings; however, we additionally noted that the higher incidence of Cfz-related RAEs might be related with the sustained irreversible proteasome inhibition as induced by Cfz and not bortezomib. Supportively, bortezomib, is a reversible inhibitor of the 26S proteasome, whereas Cfz binds irreversibly and inhibits the 20S proteasome. This difference could explain the different kidney-related side effects of these agents. Given the information from the FOCUS trial, and several more case studies reporting a comparison of Cfz with bortezomib, it appears that Cfz is more nephrotoxic than bortezomib.<sup>29,49,50</sup>

On a bench-to-bedside approach, we sought to confirm our findings in the clinical setting. We found that Cfz nephrotoxicity is manifested in patients in a similar manner as in our *in vivo* models, in compliance with the previous clinical reports on Carfilzomib-related RAEs.<sup>3</sup> For the first time we found that SGK-1 expression is significantly upregulated in patients presenting with Cfz-related nephrotoxicity, a finding that is in line with our preclinical model data. Importantly, this increase in SGK-1 expression was not correlated with serum creatinine increase, eGFR, or urine protein concentration. The lack of correlation of SGK-1 with the aforementioned biochemical (creatinine and urine protein concentration increase) and functional parameters (eGFR) is implying that SGK-1 expression might be a novel biomarker of Cfz-related nephrotoxic phenomena. Systemically increased SGK-1 is previously shown *in vivo* to be a risk factor for the development of mineralocorticoid-dependent kidney injury,<sup>51,52</sup> whereas SGK-1 expression is found to be increased in human kidneys samples with diabetes, kidney tumors, and polycystic kidney disease<sup>53</sup> and in urine and renal tubules in patients of Oxford classification T1 and T2 with IgA nephropathy.<sup>54</sup> However to the best of our knowledge this is the first time that an association of SGK-1 and Cfz-related nephrotoxic effects has been reported *in vivo* and in the clinical setting.

The fact that our clinical and preclinical data agree on the importance of MR/SGK-1 signaling in Cfz-induced

nephrotoxicity, adds to the translational value of our findings, especially when we consider the heterogeneity of toxicity in patients. The heterogeneity in patients compared to the animal models can be attributed to the variability of co-founders of renal diseases in MM patients, which are absent in the animal model. The presence and number of comorbidities, such as cardiovascular diseases, diabetes mellitus, and hypercholesterolemia are already proven to be negative predictors of renal outcome in patients with chronic kidney disease<sup>55</sup> and acute kidney injury,<sup>56</sup> as in Czf-related nephrotoxicity. Taking into consideration that MM is an elderly disease, it is to be expected that the majority of MM patients are burdened with at least 1 of the co-founders of renal diseases. This can justify the heterogeneity of the clinical in contrast to the experimental observations in animal models.

Despite the widely appreciated difficulty in directly translating preclinical data to the clinical setting, we herein managed to identify a novel druggable target, that of MR/SKG-1 axis. As mentioned above, Czf-related renal complications are common, occur acutely, are unpredictable and clinical practice requires novel approaches to fill the gap of diagnostic lack.<sup>3</sup> Monitoring of urinary rather than systemic levels of SGK-1 might be a novel and reliable tool for the identification of an early Czf-induced renal dysfunction.<sup>54</sup> However we suggest that urinary SGK-1 levels should be co-evaluated with increases in circulating NGAL and Cystatin C, already proven to be sensitive biomarkers in predicting an early-onset of renal injury in MM patients.<sup>57</sup> The importance for the co-evaluation of urinary SGK-1 and circulatory levels of NGAL and Cystatin C emerges also from the fact that NGAL expression is increased in

presence of a wide range of comorbidities such as obesity, diabetes mellitus, diabetic nephropathy,<sup>58</sup> and atherogenesis<sup>59</sup> and its polymorphisms have been shown to contribute to cardiac remodeling, fibrosis, and development of heart failure.<sup>60</sup> Thus, continuous monitoring of the patients and baseline assessment of the aforementioned sensitive markers can be considered as a clinical applicable approach, facilitating early diagnosis of Czf-related renal complications.

Furthermore, in the current study, the important role of AMPK $\alpha$  is still apparent and in agreement with our previous studies in the myocardium and aortas.<sup>4,7,61</sup> However, regarding the renal function, the mechanisms regarding AMPK $\alpha$  function and signaling are divergent from the myocardium and are closely related to transcriptional regulation of ions and molecules transporters, additionally to its effects on the metabolism and autophagy.<sup>20</sup> Despite the fact that Metformin, a clinically relevant AMPK $\alpha$  activator served as a potential prophylaxis in vivo against Czf-induced cardiotoxicity,<sup>7</sup> herein Metformin provided moderate protection against Czf-induced cytotoxicity in the prCDTECs. Moreover, since our findings indicated acute kidney injury and metabolic acidosis in the kidneys, Metformin possesses explicit contradictions in these diseases and is related to worsening of the renal complications.<sup>62</sup> Interestingly, MR antagonism emerged as a promising prophylactic intervention. Therefore, we used Eplerenone which lacks the endocrinologic side effects of spironolactone<sup>63</sup> and is widely used in patients with heart and renal failure.<sup>64</sup> Our in vitro and in vivo data presented that Eplerenone prevented Czf-related renal deficits and MR activation (Fig. 9). At the

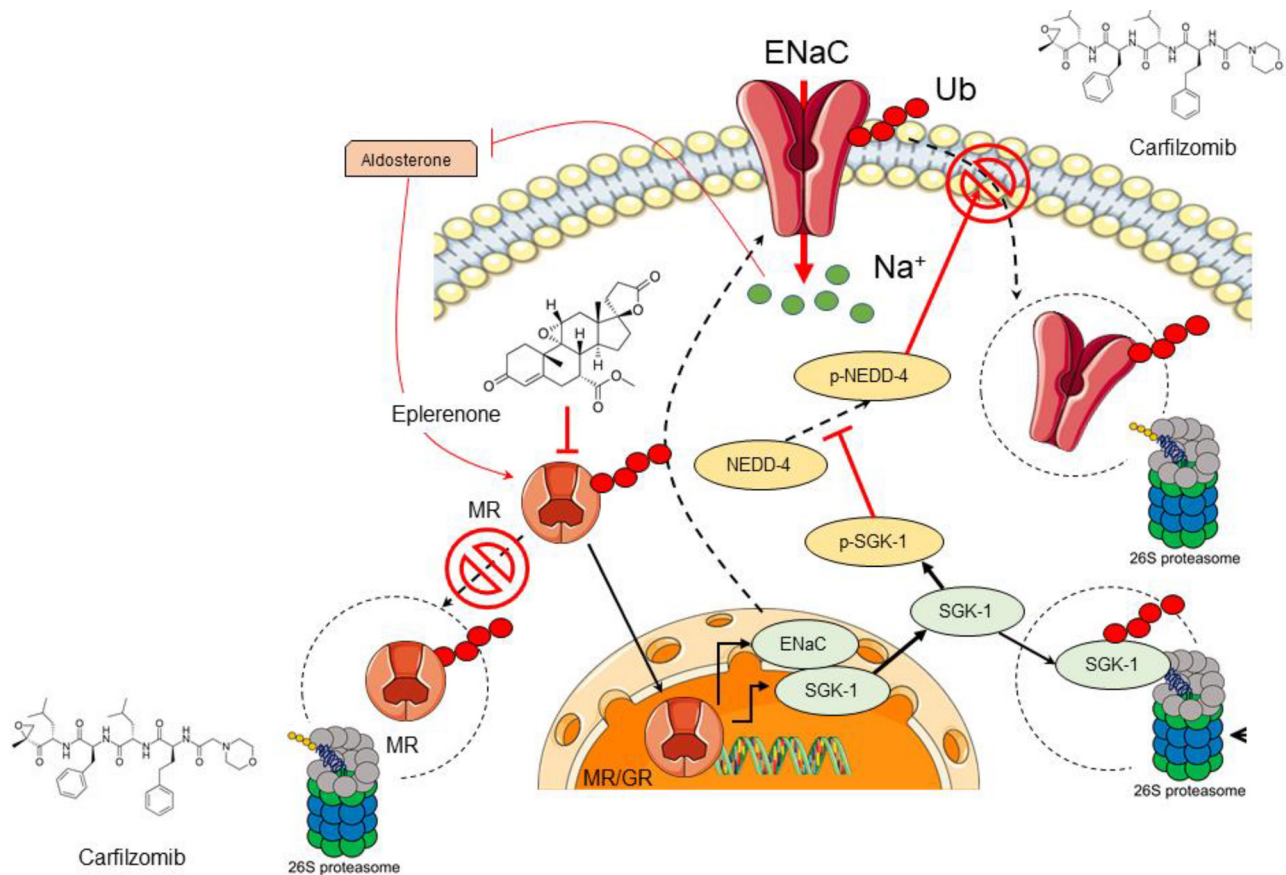


**Figure 9. Proposed Mechanism of Carfilzomib-induced nephrotoxicity.** Schematic representation of the proposed mechanism of Carfilzomib-induced hypertension and nephrotoxicity depicting the Carfilzomib-induced activation of SGK-1/MR axis and the prophylactic effect of Eplerenone. Arrows indicate activatory effects and blunted lines refer to inhibitory effects.  $\beta$ -ENaC = epithelial sodium channel 1 subunit beta; MR = mineralocorticoid receptor; Nedd4 = neural precursor expressed, developmentally down-regulated protein 4; Na<sup>+</sup> = sodium; p-SGK-1 = phospho-serum and glucocorticoid-inducible.



best of our knowledge, this is the first time that a prophylactic therapy against Cfz-related nephrotoxicity, based on clear mechanistic indications, is proposed. Despite the fact that Eplerenone, leads to a hyponatremic phenotype in the sera of the mice, Eplerenone Post-AMI Heart Failure Efficacy and Survival Study trial has proven that hyponatremia is a common mild side effect of the drug and -regardless of the plasma Na<sup>+</sup> levels- Eplerenone maintains its protective potential in patients with myocardial infarction and left ventricular dysfunction or heart failure.<sup>65</sup> Therefore, we conclude that Eplerenone exhibits a safe pharmacological profile and can serve as a safe prophylactic candidate.

Eplerenone is a MR antagonist that is widely used in patients with heart and renal failure and hypertension and presents a safe pharmacological profile with minor and rare adverse effects.<sup>66</sup> Therefore, a great percentage of the elderly MM patients would benefit from Eplerenone therapy and many of them might already have Eplerenone in their medication regimen for the management of a co-existing cardiovascular disease. The main contraindication of Eplerenone is preexisting or new-onset hyperkalemia.<sup>66</sup> Cfz therapy is associated with incidence of severe electrolyte and metabolic abnormalities including hyperkalemia, as a consequence of Cfz-induced tumor lysis syndrome.<sup>67</sup> Therefore, in patients with MM-relevant or -irrelevant hyperkalemia, close monitoring of electrolytes should be performed. Additionally, Eplerenone should be administered with caution to patients that receive Cytochrome P450 3A4 (CYP3A4) inhibitors (such as clarithromycin, erythromycin, diltiazem, itraconazole, ketoconazole, ritonavir, verapamil, etc) as the latter enzyme is the main metabolizing enzyme of Eplerenone and its inhibition is implicated with higher risk of hyperkalemia.<sup>68</sup> However, to the best of our knowledge, none of the anti-myeloma drugs belong to the CYP3A4 inhibitors category.

An additional contraindication of Eplerenone has been suggested to be the coexistence of increased urinary protein (albuminuria) and decreased creatinine clearance,<sup>69</sup> an effect that is a shared side effect with Cfz.<sup>3</sup> However, contemporary clinical studies have shown that Eplerenone exerts nephroprotective effects in patients with chronic kidney disease and diabetic nephropathy, decreasing albuminuria and improving estimated eGFR and creatinine clearance.<sup>70–72</sup> Some concerns remain about the increased risk of hyperkalemia in patients with diabetic nephropathy,<sup>73</sup> and maybe Eplerenone should be administered with caution in patients with MM and diabetic complications, as they would be the higher-risk population for manifesting hyperkalemia.

Conclusively, renal MR activation by Cfz, induces acute kidney injury, water retention, and electrolyte imbalance in vivo, while SGK-1 emerges as a possible novel biomarker of Cfz-related nephrotoxicity in the clinical setting. MR blockade by aldosterone receptor antagonist Eplerenone emerges as a potent prophylactic approach against Cfz-related nephrotoxicity; this has to be proven in patients.

#### AUTHOR CONTRIBUTIONS

PE, ET, and IA participated in the research design. PE, ET, and IA participated in the writing of the article. NK, MG, AV, NT, MAD, ET, and IA participated in reviewing and editing the manuscript. PE, SL, MM, IB, PEN, AC, CD, INS, IT, and HG participated in the performance of the research. NK, MG, AT, AV, EG, and NT contributed new reagents or analytic tools. PE, SL, MM, IB, PEN, MG, HG, AV, EG, and NT participated in the data analysis.

#### DISCLOSURES

IA, MG, MAD, and ET have received honoraria from Amgen and Janssen outside the scope of this work. ET is a HemaSphere editor. The remaining authors declare no competing financial interests.

#### REFERENCES

- Dimopoulos MA, Moreau P, Palumbo A, et al. Carfilzomib and dexamethasone versus bortezomib and dexamethasone for patients with relapsed or refractory multiple myeloma (ENDEAVOR): a randomised, phase 3, open-label, multicentre study. *Lancet Oncol.* 2016;17:27–38.
- Zamorano JL, Lancellotti P, Rodriguez Munoz D, et al. 2016 ESC position paper on cancer treatments and cardiovascular toxicity developed under the auspices of the ESC committee for practice guidelines: the task force for cancer treatments and cardiovascular toxicity of the European Society of Cardiology (ESC). *Eur Heart J.* 2016;37:2768–2801.
- Fotiou D, Roussou M, Gakiopoulou C, et al. Carfilzomib-associated renal toxicity is common and unpredictable: a comprehensive analysis of 114 multiple myeloma patients. *Blood Cancer J.* 2020;10:109.
- Eftentakis P, Kremastiotis G, Varela A, et al. Molecular mechanisms of Carfilzomib-induced cardiotoxicity in mice and the emerging cardioprotective role of metformin. *Blood.* 2019;133:710–723.
- Kilkenny C, Browne W, Cuthill IC, et al. Animal research: Reporting in vivo experiments: the ARRIVE guidelines. *Brit J Pharmacol.* 2010;160:1577–1579.
- Kilkenny C, Browne WJ, Cuthill IC, et al. Improving bioscience research reporting: the ARRIVE guidelines for reporting animal research. *Osteoarthritis Cartilage.* 2012;20:256–260.
- Eftentakis P, Varela A, Chavdoula E, et al. Levosimendan prevents doxorubicin-induced cardiotoxicity in time- and dose-dependent manner: implications for inotropy. *Cardiovasc Res.* 2020;116:576–591.
- Keidar S, Kaplan M, Pavlotzky E, et al. Aldosterone administration to mice stimulates macrophage NADPH oxidase and increases atherosclerosis development: a possible role for angiotensin-converting enzyme and the receptors for angiotensin II and aldosterone. *Circulation.* 2004;109:2213–2220.
- Levey AS, Inker LA, Coresh J. GFR estimation: from physiology to public health. *Am J Kidney Dis.* 2014;63:820–834.
- Ko GJ, Grigoryev DN, Linfert D, et al. Transcriptional analysis of kidneys during repair from AKI reveals possible roles for NGAL and KIM-1 as biomarkers of AKI-to-CKD transition. *Am J Physiol Renal Physiol.* 2010;298:F1472–F1483.
- Hoy WE, Bertram JF, Denton RD, et al. Nephron number, glomerular volume, renal disease and hypertension. *Curr Opin Nephrol Hypertens.* 2008;17:258–265.
- Troxell ML, Scandling JD, Sibley RK. Renal juxtaglomerular apparatus hyperplasia. *Nephrol Dial Transplant.* 2005;20:2282–2283.
- Shang J, Zhao Z. Emerging role of HuR in inflammatory response in kidney diseases. *Acta Biochim Biophys Sin (Shanghai).* 2017;49:753–763.
- Heinolainen K, Karaman S, D'Amico G, et al. VEGFR3 Modulates vascular permeability by controlling VEGF/VEGFR2 signaling. *Circ Res.* 2017;120:1414–1425.
- Sadler JE. Von Willebrand factor, ADAMTS13, and thrombotic thrombocytopenic purpura. *Blood.* 2008;112:11–18.
- Izzi B, Gialluisi A, Gianfagna F, et al. Platelet distribution width is associated with P-selectin dependent platelet function: results from the Moli-family cohort study. *Cells.* 2021;10:2737.
- Tsai HM. The molecular biology of thrombotic microangiopathy. *Kidney Int.* 2006;70:16–23.
- Chesney RW, Han X, Patters AB. Taurine and the renal system. *J Biomed Sci.* 2010;17:54.
- Hanifa MA, Skott M, Maltesen RG, et al. Tissue, urine and blood metabolite signatures of chronic kidney disease in the 5/6 nephrectomy rat model. *Metabolomics.* 2019;15:112.
- Glosse P, Foller M. AMP-Activated Protein Kinase (AMPK)-dependent regulation of renal transport. *Int J Mol Sci.* 2018;19:3481.
- Bankir L, Bichet DG, Bouby N. Vasopressin V2 receptors, ENaC, and sodium reabsorption: a risk factor for hypertension? *Am J Physiol Renal Physiol.* 2010;299:F917–F928.
- Mamazhakypov A, Hein L, Lothar A. Mineralocorticoid receptors in pulmonary hypertension and right heart failure: from molecular biology to therapeutic targeting. *Pharmacol Ther.* 2021;231:107987.
- Bauersachs J, Jaissner F, Toto R. Mineralocorticoid receptor activation and mineralocorticoid receptor antagonist treatment in cardiac and renal diseases. *Hypertension.* 2015;65:257–263.
- Calhoun DA. Fluid retention, aldosterone excess, and treatment of resistant hypertension. *Lancet Diabetes Endocrinol.* 2018;6:431–433.
- Stubblefield E, Mueller GC. Effects of Sodium Chloride Concentration on Growth, Biochemical Composition, and Metabolism of HeLa Cells\*. *Cancer Res.* 1960;20:1646–1655.

26. Bize V, Horisberger JD. Sodium self-inhibition of human epithelial sodium channel: selectivity and affinity of the extracellular sodium sensing site. *Am J Physiol Renal Physiol*. 2007;293:F1137–F1146.
27. Xiao J, Shimada M, Liu W, et al. Anti-inflammatory effects of eplerenone on viral myocarditis. *Eur J Heart Fail*. 2009;11:349–353.
28. Bringham S, Milan A, D'Agostino M, et al. Prevention, monitoring and treatment of cardiovascular adverse events in myeloma patients receiving Carfilzomib a consensus paper by the European Myeloma Network and the Italian Society of Arterial Hypertension. *J Intern Med*. 2019;286:63–74.
29. Chari A, Hajje D. Case series discussion of cardiac and vascular events following Carfilzomib treatment: possible mechanism, screening, and monitoring. *BMC Cancer*. 2014;14:915.
30. Rosenthal A, Luthi J, Belohlavek M, et al. Carfilzomib and the cardiorenal system in myeloma: an endothelial effect? *Blood Cancer J*. 2016;6:e384.
31. Wang YN, Hu HH, Zhang DD, et al. The dysregulation of eicosanoids and bile acids correlates with impaired kidney function and renal fibrosis in chronic renal failure. *Metabolites*. 2021;11:127.
32. Zhao YY, Wang HL, Cheng XL, et al. Metabolomics analysis reveals the association between lipid abnormalities and oxidative stress, inflammation, fibrosis, and Nrf2 dysfunction in aristolochic acid-induced nephropathy. *Sci Rep*. 2015;5:12936.
33. van de Poll MC, Soeters PB, Deutz NE, et al. Renal metabolism of amino acids: its role in interorgan amino acid exchange. *Am J Clin Nutr*. 2004;79:185–197.
34. Belova L, Sharma S, Brickley DR, et al. Ubiquitin-proteasome degradation of serum- and glucocorticoid-regulated kinase-1 (SGK-1) is mediated by the chaperone-dependent E3 ligase CHIP. *Biochem J*. 2006;400:235–244.
35. Faresse N, Ruffieux-Daidie D, Salamin M, et al. Mineralocorticoid receptor degradation is promoted by Hsp90 inhibition and the ubiquitin-protein ligase CHIP. *Am J Physiol-Renal*. 2010;299:F1462–F1472.
36. Malik B, Schlanger L, Al-Khalili O, et al. ENaC degradation in A6 cells by the ubiquitin-proteasome proteolytic pathway. *J Biol Chem*. 2001;276:12903–12910.
37. Yokota K, Shibata H, Kobayashi S, et al. Proteasome-mediated mineralocorticoid receptor degradation attenuates transcriptional response to aldosterone. *Endocr Res*. 2004;30:611–616.
38. Al-Harbi NO, Imam F, Al-Harbi MM, et al. Rutin inhibits Carfilzomib-induced oxidative stress and inflammation via the NOS-mediated NF-kappaB signaling pathway. *Inflammopharmacology*. 2019;27:817–827.
39. Jhaveri KD, Chidella S, Varghese J, et al. Carfilzomib-related acute kidney injury. *Clin Adv Hematol Oncol*. 2013;11:604–605.
40. Jhaveri KD, Wanchoo R. Carfilzomib-induced nephrotoxicity. *Kidney Int*. 2015;88:199–200.
41. Sullivan MR, Danilov AV, Lansigan F, et al. Carfilzomib associated thrombotic microangiopathy initially treated with therapeutic plasma exchange. *J Clin Apher*. 2015;30:308–310.
42. Wanchoo R, Khan S, Koltz JE, et al. Carfilzomib-related acute kidney injury may be prevented by N-acetyl-L-cysteine. *J Oncol Pharm Pract*. 2015;21:313–316.
43. Bertocchio JP, Warnock DG, Jaisser F. Mineralocorticoid receptor activation and blockade: an emerging paradigm in chronic kidney disease. *Kidney Int*. 2011;79:1051–1060.
44. Alchi B, Shirasaki A, Narita I, et al. Renovascular hypertension: a unique cause of unilateral focal segmental glomerulosclerosis. *Hypertens Res*. 2006;29:203–207.
45. Gyuraszova M, Kovalcikova AG, Renczes E, et al. Oxidative stress in animal models of acute and chronic renal failure. *Dis Markers*. 2019;2019:8690805.
46. Nagase M, Ayuzawa N, Kawarazaki W, et al. Oxidative stress causes mineralocorticoid receptor activation in rat cardiomyocytes: role of small GTPase Rac1. *Hypertension*. 2012;59:500–506.
47. Kim YG, Suga SI, Kang DH, et al. Vascular endothelial growth factor accelerates renal recovery in experimental thrombotic microangiopathy. *Kidney Int*. 2000;58:2390–2399.
48. Mansley MK, Korbmacher C, Bertog M. Inhibitors of the proteasome stimulate the epithelial sodium channel (ENaC) through SGK1 and mimic the effect of aldosterone. *Pflugers Arch*. 2018;470:295–304.
49. Hajek R, Maszi T, Petrucci MT, et al. A randomized phase III study of Carfilzomib vs low-dose corticosteroids with optional cyclophosphamide in relapsed and refractory multiple myeloma (FOCUS). *Leukemia*. 2017;31:107–114.
50. Wanchoo R, Abudayyeh A, Doshi M, et al. Renal toxicities of novel agents used for treatment of multiple myeloma. *Clin J Am Soc Nephrol*. 2017;12:176–189.
51. Sierra-Ramos C, Velazquez-Garcia S, Keskus AG, et al. Increased SGK1 activity potentiates mineralocorticoid/NaCl-induced kidney injury. *Am J Physiol Renal Physiol*. 2021;320:F628–F643.
52. Farjah M, Roxas BP, Geenen DL, et al. Dietary salt regulates renal SGK1 abundance: relevance to salt sensitivity in the Dahl rat. *Hypertension*. 2003;41:874–878.
53. Kumar JM, Brooks DP, Olson BA, et al. Sgk, a putative serine/threonine kinase, is differentially expressed in the kidney of diabetic mice and humans. *J Am Soc Nephrol*. 1999;10:2488–2494.
54. Lu X, Li M, Zhou L, et al. Urinary serum- and glucocorticoid-inducible kinase SGK1 reflects renal injury in patients with immunoglobulin A nephropathy. *Nephrology (Carlton)*. 2014;19:307–317.
55. Lee WC, Lee YT, Li LC, et al. The number of comorbidities predicts renal outcomes in patients with stage 3(-)5 chronic kidney disease. *J Clin Med*. 2018;7:493.
56. Pereira MB, Zanetta DM, Abdulkader RC. The real importance of pre-existing comorbidities on long-term mortality after acute kidney injury. *PLoS One*. 2012;7:e47746.
57. Papassotiriou GP, Kastritis E, Gkatzamanidou M, et al. Neutrophil gelatinase-associated lipocalin and cystatin C are sensitive markers of renal injury in patients with multiple Myeloma. *Clin Lymphoma Myeloma Leuk*. 2016;16:29–35.
58. Lang F, Gorch A, Vallon V. Targeting SGK1 in diabetes. *Expert Opin Ther Targets*. 2009;13:1303–1311.
59. Borst O, Schaub M, Walker B, et al. Pivotal role of serum- and glucocorticoid-inducible kinase 1 in vascular inflammation and atherogenesis. *Arterioscler Thromb Vasc Biol*. 2015;35:547–557.
60. Han W, Zhang H, Gong X, et al. Association of SGK1 polymorphisms with susceptibility to coronary heart disease in Chinese Han patients with comorbid depression. *Front Genet*. 2019;10:921.
61. Efentakis P, Psarakou G, Varela A, et al. Elucidating Carfilzomib's induced cardiotoxicity in an in vivo model of aging: prophylactic potential of metformin. *Int J Mol Sci*. 2021;22:10956.
62. Connelly PJ, Lonergan M, Soto-Pedre E, et al. Acute kidney injury, plasma lactate concentrations and lactic acidosis in metformin users: a GoDarts study. *Diabetes Obes Metab*. 2017;19:1579–1586.
63. Manolis AA, Manolis TA, Melita H, et al. Eplerenone Versus Spironolactone in Resistant Hypertension: an Efficacy and/or Cost or Just a Men's Issue? *Curr Hypertens Rep*. 2019;21:22.
64. Pitt B, Pedro Ferreira J, Zannad F. Mineralocorticoid receptor antagonists in patients with heart failure: current experience and future perspectives. *Eur Heart J Cardiovasc Pharmacother*. 2017;3:48–57.
65. Martens P, Ferreira JP, Vincent J, et al. Serum sodium and eplerenone use in patients with a myocardial infarction and left ventricular dysfunction or heart failure: insights from the EPHEUS trial. *Clin Res Cardiol*. 2021.
66. Struthers A, Krum H, Williams GH. A comparison of the aldosterone-blocking agents eplerenone and spironolactone. *Clin Cardiol*. 2008;31:153–158.
67. Harvey RD. Incidence and management of adverse events in patients with relapsed and/or refractory multiple myeloma receiving single-agent Carfilzomib. *Clin Pharmacol*. 2014;6:87–96.
68. Moore TD, Nawarskas JJ, Anderson JR. Eplerenone: a selective aldosterone receptor antagonist for hypertension and heart failure. *Heart Dis*. 2003;5:354–363.
69. Hughes JC, Cassagnol M. *Eplerenone*. In: *StatPearls*. Treasure Island, Florida, USA: StatPearls Publishing;2022.
70. Epstein M, Williams GH, Weinberger M, et al. Selective aldosterone blockade with eplerenone reduces albuminuria in patients with type 2 diabetes. *Clin J Am Soc Nephrol*. 2006;1:940–951.
71. Hu H, Zhao X, Jin X, et al. Efficacy and safety of eplerenone treatment for patients with diabetic nephropathy: a meta-analysis. *PLoS One*. 2022;17:e0265642.
72. Patel V, Joharapurkar A, Jain M. Role of mineralocorticoid receptor antagonists in kidney diseases. *Drug Dev Res*. 2021;82:341–363.
73. Barrera-Chimal J, Lima-Posada I, Bakris GL, et al. Mineralocorticoid receptor antagonists in diabetic kidney disease - mechanistic and therapeutic effects. *Nat Rev Nephrol*. 2022;18:56–70.